ACS OMEGA

http://pubs.acs.org/journal/acsodf

Article

# Specificity of Monoterpene Interactions with Insect Octopamine and Tyramine Receptors: Insights from *in Silico* Sequence and Structure Comparison

Almira B. Ocampo, Joseph Gregory Z. Cabinta, Hyvi Valerie J. Padilla, Eizadora T. Yu, and Ricky B. Nellas*

Cite This: *ACS Omega* 2023, 8, 3861−3871

Read Online

ACCESS | Metrics & More | Article Recommendations | Supporting Information

**ABSTRACT:** Octopamine and tyramine receptors (OARs/TARs) are interesting targets for new insecticide development due to their unique roles in insects' physiological and cellular response and their specificity to invertebrates. Monoterpene compounds that bear resemblance to the natural ligands have been shown to bind to the OARs/TARs but elicit varied responses in different insect species. Using *in silico* methods, we attempt to investigate the molecular basis of monoterpene interactions and their specificity in different OARs and TARs of damaging or beneficial insects. Sequence and structure comparison revealed that the OARs/TARs studied generally have more similarities in terms of structure rather than sequence identity. Together with clustering and network analyses, we also revealed that the role of IL3 might be crucial in the identification of OAR and TAR and their unique function. Among the 35 monoterpenes subjected to ensemble docking, carvacrol had the most negative average binding energies with the target insect OARs and TARs. The differences in the key interacting residues of carvacrol with insect OARs and TARs could be the origin of variation in the responses of insect species to this monoterpene. Results suggest that carvacrol may be a potential natural-product-based insecticide, targeting multiple insect pests while being nonharmful to honeybees and Asian swallowtail butterflies. This work could provide insights into the development of effective species-specific natural-product-based insecticides that are more environmentally friendly than conventional insecticides.

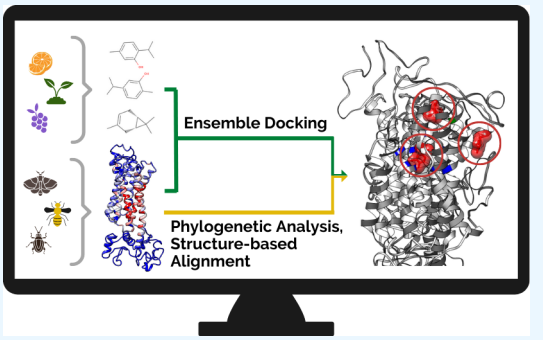


## INTRODUCTION

The need to feed a growing world population is driving the demand for better pest management and agricultural practices. The continuous push for the discovery of next-generation pesticides stems from the need for products that (1) are more environmentally friendly, (2) are less toxic to nontargets, (3) satisfy current agricultural needs, and (4) address insecticide resistance.[1,2] Insecticides with different modes of action are good alternatives to bypass the resistance of some pests to conventional insecticides.[2]

One of the targets that has gained interest in the discovery of new insecticides is the arthropod G-protein-coupled receptors (GPCRs).[2] GPCRs are known for their critical role in insect physiological functions.[3] Triggered by binding of extracellular ligands, these receptors transfer signals to intracellular signaling proteins, which regulate a diverse array of intracellular signaling cascades.[2,4] Among the arthropod GPCRs, the insect octopaminergic receptors have attracted attention for new insecticide discovery due to the specificity of the octopaminergic pathway to arthropods and their crucial roles in insect physiology and cellular response.[2,5] Octopamine and tyramine receptors (OARs and TARs, respectively) are under the Class A GPCR classification. OARs are classified into three groups, namely: (1) $\alpha$-adrenergic-like octopamine receptors (OAR1); (2) $\beta$-adrenergic-like octopamine receptors (OAR2); and (3) octopamine/tyramine receptors (TyrR).[6] It was later found that tyramine (TA) has an independent biological function from octopamine (OA) in insect physiological functions such as locomotion and reproduction.[7]

Insect pests are the primary source of biotic stress on crops which can greatly reduce agricultural production and food supply.[8] An example is the cabbage moth, *Mamestra brassicae*, that has been reported as a damaging pest of *Brassica* vegetables throughout Asia and Europe.[9] The Malaysian fruit fly, *Bactrocera latifrons*, was found to have a host range of at least 15 plant species in the families Solanaceae and Cucurbitaceae in Hawaii.[10] However, not all insects are pests as some insects are useful to plants and humans.[11] An example

Received: September 28, 2022
Accepted: December 28, 2022
Published: January 13, 2023

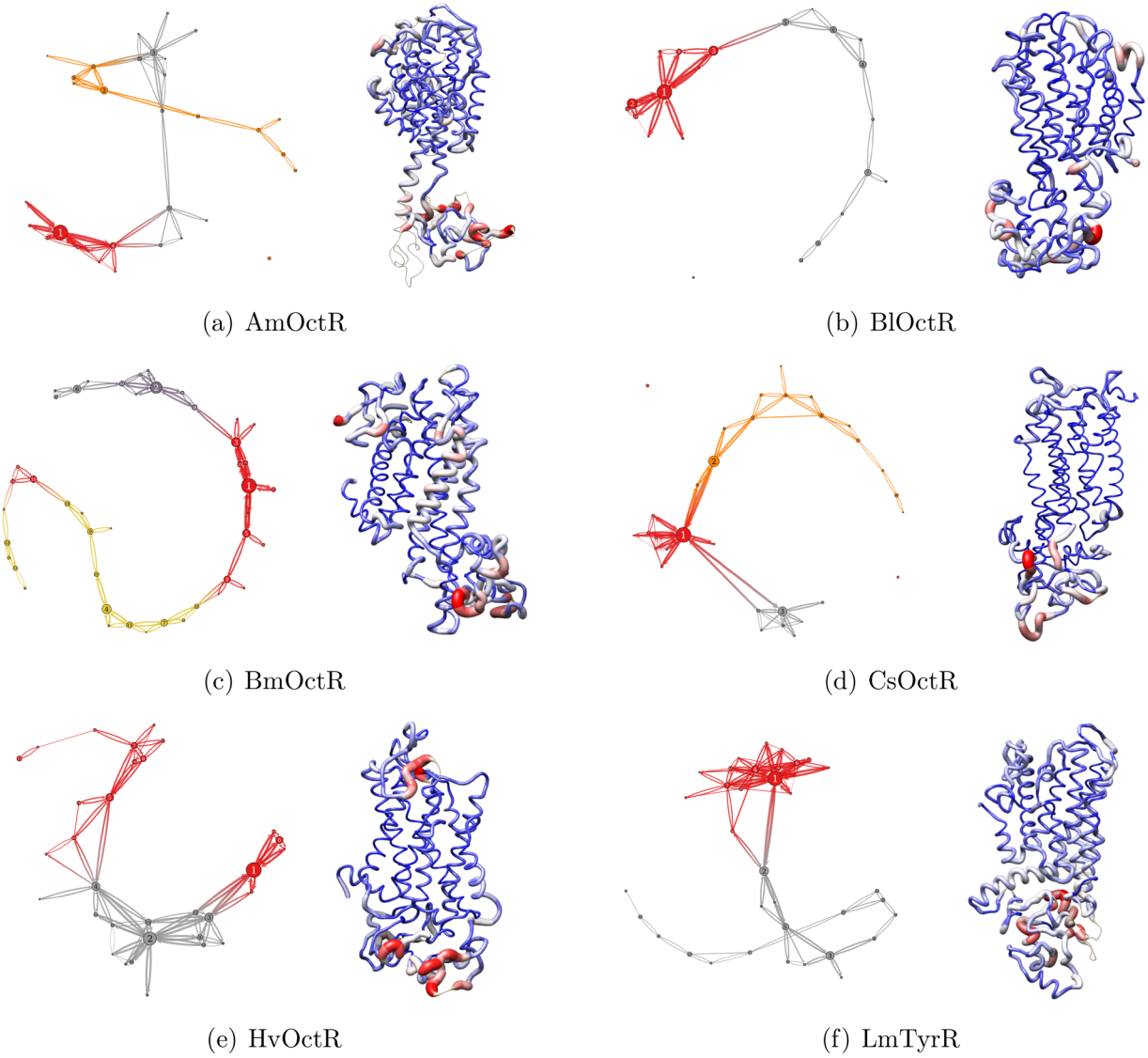


**Figure 1.** Left: Network representations of conformational transitions of AmOctR, BlOctR, BmOctR, CsOctR, HvOctR, and LmTyr. Right: Superimposition of nodes 1 and 2 where the thickness of the worm depicts the RMSD value and colors blue, white, and red depict relatively low, moderate, and high RMSD values, respectively.

is the honey bee (*Apis mellifera*, L.) which is known to be the most important pollinating insect species and plays a vital role in the world's agriculture. This beneficial insect assists in the pollination of a wide variety of crops and produces honey and other hive products.[12] Common to both damaging and beneficial insects is the presence of OA and TA, which are the invertebrate counterparts of adrenaline and noradrenaline in mammals.[13] Although OA and TA receptors are structurally similar to vertebrate adrenergic receptors, the pharmacological characteristics are different. OARs and TARs are uniquely active in invertebrates, and targets of these receptors would show negligible toxicity to vertebrates.[13] This makes OA and TA receptors ideal targets for highly specific insecticides.[14]

Essential oil constituents such as monoterpenes have been shown to target arthropod proteins such as acetylcholinesterase (ACHE) and octopaminergic and tyraminergic receptors to induce neuromodulatory and neurotoxicity effects.[15−20] Among plant secondary metabolites, monoterpenes have been widely studied and are considered as environmentally friendly and safe alternatives to conventional synthetic insecticides.[21] Although observed to possess biological activities with OARs and TARs, monoterpenes exhibit different pharmacological effects in different insects. For example, some monoterpenes such as carvacrol exhibited an agonist effect on the type 1 tyramine receptor (TAR1) of the fruit fly, *Drosophila melanogaster*.[22] Carvacrol also induces a positive allosteric modulation on TAR1 of the cattle tick, *Rhipicephalus (Boophilus) microplus*, and fruit fly, *Drosophila suzukii*.[23,24] Moreover, a study demonstrated that structurally related plant monoterpenoids possess different toxic activities through their action against the OARs of *Periplaneta americana* and *Drosophila melanogaster*.[22] Different monoterpene structures have also been observed to elicit different responses in insect species. Oxygenated monoterpenes and terpenoids such as pulegone have also been shown to have high contact toxicity to rice weevil (*Sitophilus oryzae*).[25] They are suggested to enhance receptor interaction, acting as agonists of the tyramine receptor of *D. melanogaster* and *R. microplus*.[22,23] Oxygenated monoterpenes have also been observed to have higher


https://doi.org/10.1021/acsomega.2c06256
ACS Omega 2023, 8, 3861−3871

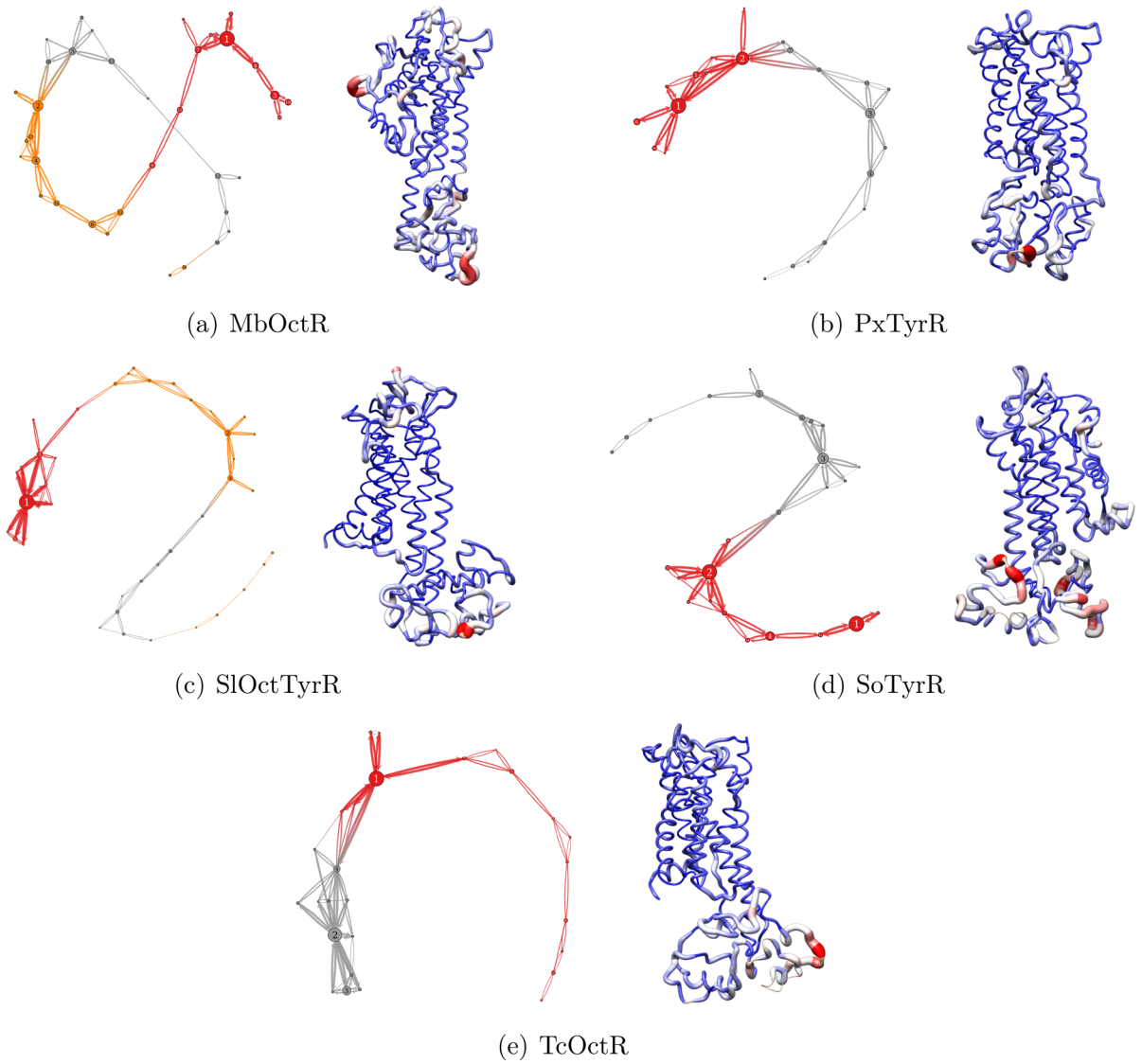


**Figure 2.** Left: Network representations of conformational transitions of MbOctR, PxTyR, SlOctTyR, SoTyR, and TcOctR. Right: Superimposition of nodes 1 and 2 where the thickness of the worm depicts the RMSD value and colors blue, white, and red depict relatively low, moderate, and high RMSD values, respectively.

antitermitic activities to the Japanese termite *Reticulitermes speratus* Kolbe than their nonoxygenated analogues.[26]

Although different monoterpenes have been established to have toxicity and repellency effects in different insect species, the biochemical mechanism has not been fully deduced. In this study, we attempt to investigate the specificity of the binding of monoterpenes to OARs/TARs from 11 different insect species: *Apis mellifera*, *Bactrocera latifrons*, *Bombyx mori*, *Chilo suppressalis*, *Heliothis virescens*, *Locusta migratoria*, *Mamestra brassicae*, *Papilio xuthus*, *Spodoptera littoralis*, *Sitophilus oryzae*, and *Tribolium castaneum*. Using *in silico* tools, the sequence and structure similarities and differences of their OARs/TARs and their interactions with monoterpene compounds were explored. Agrochemical research using recent *in silico* tools are currently being explored due to the growing advances in technology and improvement of existing techniques, contributing to their wide application.[1]

## RESULTS AND DISCUSSION

**Homology Modeling.** In the absence of crystal structures, the 3D models of the 11 insect receptors, *A. mellifera* OAR (AmOctR), *B. latifrons* OAR (BlOctR), *B. mori* OAR (BmOctR), *C. suppressalis* OAR (CsOctR), *H. virescens* OAR (HvOctR), *L. migratoria* TAR (LmTyrR), *M. brassicae* OAR (MbOctR), *P. xuthus* TAR (PxTyrR), *S. littoralis* OAR/TAR (SlOctTyrR), *S. oryzae* TAR (SoTyrR), and *T. castaneum* OAR (TcOctR), were obtained using I-TASSER.[27] These models have C-scores ranging from −2.58 to −0.72 and TM (template-modeling)-score values ranging from 0.42 ± 0.15 to 0.62 ± 0.14 (Table S1). The C-score is the confidence score of the predicted models, and a value of −1.5 or higher denotes reasonable folding of the protein.[27] Furthermore, a TM-score value of <0.17 indicates high similarity between two randomly selected structures from the PDB library, and a TM-score value of >0.5 indicates a model of reasonable topology.[27] The models have 17−45% sequence identities when aligned and compared to the template sequences used. Although some C-score values were low, which can be attributed to the low



https://doi.org/10.1021/acsomega.2c06256
ACS Omega 2023, 8, 3861−3871

sequence similarity between the input and template sequences, the TM-score values suggest that the models represent reasonable topology and structural prediction of the receptors.[27,28] A relatively low similarity in terms of sequence identity compared to secondary structure is a general characteristic of GPCRs.[29,30]

**Clustering and Network Analysis.** The network analysis representations of each OAR/TAR conformational transition are shown in Figure 1 and Figure 2. Root-mean-square-distance (RMSD)-based clustering analysis using the algorithm described by Daura et al. was used to group similar protein conformations into one representative structure, which makes one node of the network.[31] Each node represents a local minimum in the energy landscape, and the edges represent the transitions connecting each minima.[32] The size of the node corresponds to the number of clustered protein conformations and, thus, corresponds to the frequency at which a conformation is visited throughout the simulation. Each distinct partition state distribution is represented by a different color in the network representation. For all the OARs/TARs, two to four partition states were observed. Using the superimposed structures of the two largest nodes of each OAR/TAR, a common trend observed was the relatively large RMSD values of the extracellular (EL) and intracellular (IL) domains compared to the transmembrane (TM) domains, which implies prominent motion in the non-TM regions. Notably, among the domains, the highest RMSD values were generally in the IL3 domain of each OAR/TAR.

**Sequence and Structure Comparison.** Figure 3 shows the phylogenetic tree obtained from aligning the 11 insect OARs/TARs and reveals evolutionary relationships between these proteins. *A. mellifera* OAR is distinctly different from the other OARs/TARs. It also shows which OAR/TAR proteins are more related to each other. An example is the OARs/TARs from the rice weevil, Asiatic rice borer, and red-flour beetle that are clustered together.

With regard to the secondary structure alignment (Table S2), CsOctR was used as the reference structure in the superimposition of secondary structures of all receptors since it produced the highest C-score and TM-score from homology modeling. Pruned atom pairs refer to the atoms of the receptor that aligned with the secondary structure of CsOctR. The root-mean-square deviation (RMSD) is calculated from the backbone $C^{\alpha}$ of the residues. The number of aligned residues (pruned atom pairs) is highest when CsOctR is matched with SoTyrR and TcOctR. In contrast, the total atom pair RMSD is highest when CsOctR is compared with HvOctR. These results correlate with the phylogenetic analysis (Figure 3) wherein CsOctR, SoTyrR, and TcOctR are grouped together, while HvOctR is positioned in a distant group. *C. suppresalis*, *S. oryzae*, and *T. castaneum* are all considered as major storage and grain insect pests.[33]

On the other hand, AmOctR alignment with SoTyrR had the highest RMSD of 2.672 Å (Table S3). This correlates with the phylogenetic analysis, wherein the results showed that AmOctR and SoTyrR are members of different and distant families. However, the RMSD value is still close to the optimal RMSD cutoff applied in determining similar 3D conformations in the performed clustering analysis (2.0−2.5 Å). Together with homology modeling results, these findings generally suggest that the OARs/TARs have higher similarity in terms of structure rather than sequence identity.

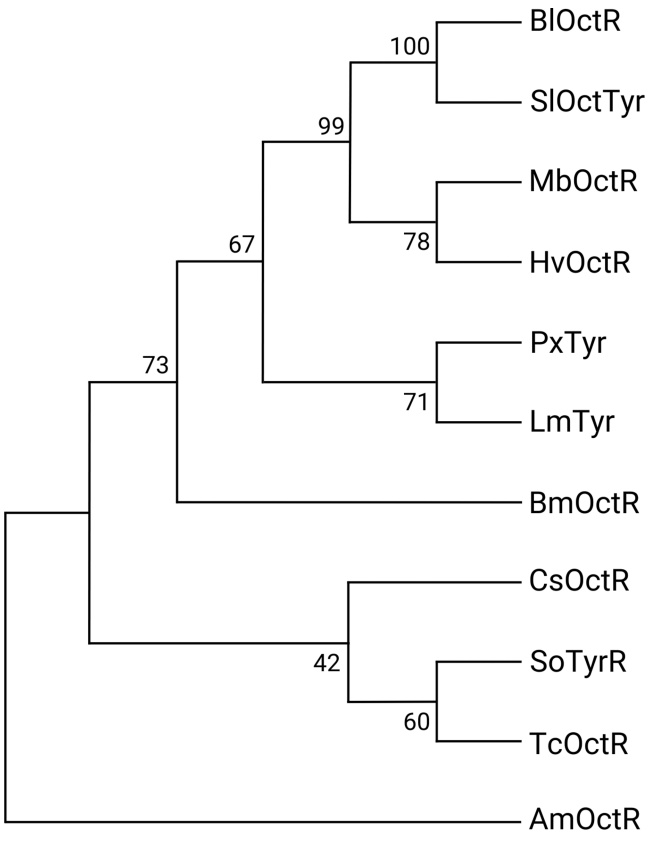


**Figure 3.** Phylogenetic tree of the 11 insect OAR/TAR protein sequences. The phylogenetic tree was constructed using the Maximum Likelihood method. The number for each node is the bootstrap percentage.

Among the domains, it was observed from the secondary structure-based sequence alignment that the IL3 region had the most gaps and amino acid variations among the OARs and TARs. AmOctR has the farthest sequence correlation among the OARs/TARs investigated, and it was also observed to have the longest IL3 with 188 amino acids (the rest of the receptors ranging from 158 to 177 residues). In a separate study, the *A. mellifera* TAR1 receptor (*Amtyr1*) was observed to have a relatively shorter IL3 compared to other TAR1 receptors which can be related to the fact that this GPCR couples only with the Gi protein and not with Gq upon activation.[34] Along with the findings from network analysis, our results suggest that IL3 structure, length, and sequence might be crucial for each OAR and TAR identification, activation, and unique function. The IL3 region is seen to have no effect prior to ligand binding but is suggested to play a crucial role in OAR/TAR activation mechanisms that occur after ligand binding.[35,36]

The secondary-structure-based multiple sequence alignment (Figure S1) revealed the conserved regions among all 11 receptors. Figure 4 shows a representative structure based on the superimposition rendered by conservation using the multiple sequence alignment. In general, the OARs and TARs have very low structure-based sequence similarities (colored in blue) especially in the extracellular and intracellular loops. Among the loops, the intracellular loop 2 (IL2) has the highest number of conserved residues. Transmembranes 3, 5, and 6 (TM3, TM5, and TM6) contain regions that have moderate (colored in white) to high (colored in red) sequence


https://doi.org/10.1021/acsomega.2c06256
ACS Omega 2023, 8, 3861−3871

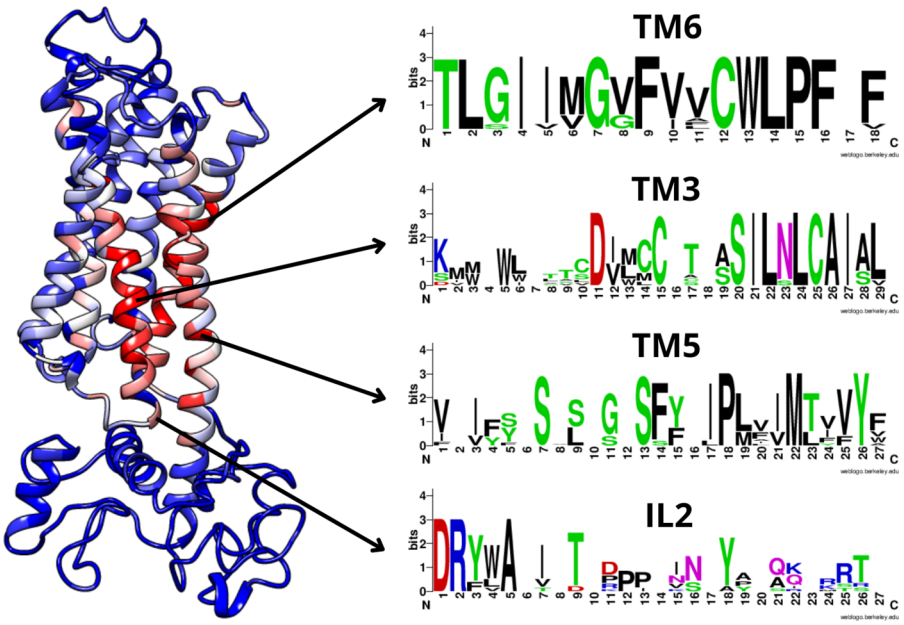


**Figure 4.** Representative structure from the superimposition of the 11 insect receptors rendered by conservation, 1 as highly conserved and 0 as no conservation observed (blue: 0.09; white: 0.55; red: 1.00).

similarity. From the network analysis, less dominant motions are also generally observed in the TM regions where the endogenous ligands bind. The common GPCR molecular switches observed in previous studies are also seen aligned and conserved.[37−40] The highly conserved DRY (Asp-Arg-Tyr) and CWxxP (Cys-Trp-x-x-Pro) motifs are located in IL2 (downstream of TM3) and TM6, respectively. These motifs are highly conserved in Class A GPCRs and are associated in regulating GPCR inactive and active conformational states, making these residues critical for receptor function.[37−40]

**Ensemble Docking.** To assess the potential of monoterpenes to bind with the receptors and evaluate their key interactions, ensemble docking was employed. Identifying and investigating the key receptor residues that interact with different ligands is a step toward the elucidation of ligand specificity and receptor activation. In previous studies, it was observed that majority of Class A GPCRs make consensus contacts with residues at positions 3.32, 3.33, 3.36, 6.48, 6.51, and 7.39 in the orthosteric pocket (Table S4 and Table S5 for Ballesteros−Weinstein naming guides).[40−42] A majority of these residues are tagged as conserved from the structural alignment, which shows the similarity of the orthosteric pocket position among the receptors.

Aside from the monoterpenes, the endogenous ligands were also docked to serve as control systems. Using OA and TA docking results, the preference for (*R*)-octopamine over (*S*)-octopamine was observed in the majority of the OARs. However, it is observed that molecular docking is not enough to distinguish the TAR endogenous ligand preference, as OA had higher binding affinities (most negative binding energies in kcal/mol) compared to TA even for TARs as shown in Table 1.

The top hits and most negative average binding energies in kcal/mol are presented in Table 2. The top hits refer to the monoterpenes that had the most negative binding energies in one receptor conformation, while the most negative average binding energies are defined as the averages of the binding energies obtained from all receptor conformations. The

**Table 1. Binding Energies of Endogenous Ligand Ensemble Docking Reported as Average Binding Energy with Standard Deviation in kcal/mol**

| | Endogenous Ligand | | |
|---|---|---|---|
| Receptor | (*S*)-Octopamine | (*R*)-Octopamine | Tyramine |
| AmOctR | −3.44 ± 1.43 | −3.55 ± 1.41 | −3.75 ± 0.99 |
| BlOctR | −4.63 ± 0.79 | −4.67 ± 0.78 | −4.77 ± 0.60 |
| BmOctR | −4.74 ± 0.90 | −4.73 ± 0.92 | −4.77 ± 0.91 |
| CsOctR | −4.50 ± 0.73 | −5.10 ± 0.68 | −4.50 ± 0.68 |
| HvOctR | −3.60 ± 0.65 | −3.68 ± 0.69 | −3.63 ± 0.60 |
| LmTyrR | −5.49 ± 0.54 | −5.45 ± 0.54 | −5.45 ± 0.49 |
| MbOctR | −5.60 ± 0.36 | −5.63 ± 0.36 | −5.48 ± 0.33 |
| PxTyrR | −4.73 ± 0.63 | −4.78 ± 0.63 | −4.68 ± 0.62 |
| SlOctTyrR | −3.94 ± 0.81 | −4.04 ± 0.75 | −4.11 ± 0.79 |
| SoTyrR | −5.55 ± 0.24 | −5.57 ± 0.23 | −5.30 ± 0.22 |
| TcOctR | −3.88 ± 0.59 | −3.92 ± 0.58 | −3.89 ± 0.58 |

monoterpene binding energies are generally significantly higher than those of the endogenous ligands which highlights the potential of monoterpenes as ligands for OARs and TARs. Carene, pulegone, carvacrol, terpinolene, and thymol are determined to be top hits to more than one OAR/TAR. Four of these monoterpenes are also classified as top hits in the ensemble docking of SoTyrR in a separate study.[15] On the other hand, top hits sabinene and camphene are unique to HvOctR; (+)-3-bromocamphor is unique to PxTyrR; and B-camphol is unique to SoTyrR. This may suggest that these monoterpenes have potential species-specific action through the OARs/TARs of *H. virescens*, *P. xuthus*, and *S. oryzae*. Further studies are necessary as it was observed in just one receptor conformation.

Interestingly, carvacrol had the most negative average binding energy in all of the systems except for MbOctR, where it ranked second to pulegone. Common close-interacting residues for all the carvacrol interactions were determined. A common close-interacting residue is determined if the distance between atoms of receptor residues and the


https://doi.org/10.1021/acsomega.2c06256
ACS Omega 2023, 8, 3861−3871

**Table 2. Monoterpene Top Hits versus the Endogenous Ligand Binding Energies**

| Receptor | Monoterpene Top Hits | Most Negative Binding Energy (kcal/mol) | Monoterpene Top Hits (Average) | Most Negative Average Binding Energy (kcal/mol) | Endogenous Ligand | Average Binding Energy (kcal/mol) |
|---|---|---|---|---|---|---|
| AmOctR | (+)-3-Carene | −6.70 | Carvacrol | −5.65 ± 0.41 | OA | −3.55 ± 1.41 |
| | Pulegone | −6.70 | | | | |
| BlOctR | Carene | −7.20 | Carvacrol | −5.94 ± 0.53 | OA | −4.67 ± 0.78 |
| | Thymol | −7.20 | | | | |
| BmOctR | Pulegone | −7.60 | Carvacrol | −5.82 ± 0.54 | OA | −4.73 ± 0.92 |
| CsOctR | Pulegone | −7.20 | Carvacrol | −5.75 ± 0.52 | OA | −5.10 ± 0.68 |
| HvOctR | Sabinene | −6.90 | Carvacrol | −5.51 ± 0.32 | OA | −3.68 ± 0.69 |
| | Camphene | −6.90 | | | | |
| LmTyrR | Pulegeone | −7.70 | Carvacrol | −5.76 ± 0.58 | TA | −5.45 ± 0.49 |
| MbOctR | Pulegeone | −7.50 | Pulegone | −6.45 ± 0.52 | OA | −5.63 ± 0.36 |
| | Thymol | −7.50 | | | | |
| | Terpinolene | −7.50 | | | | |
| PxTyrR | (+)-3-Bromo-camphor | −7.50 | Carvacrol | −5.75 ± 0.56 | TA | −4.68 ± 0.62 |
| SlOctTyrR | (+)-3-Carene | −7.30 | Carvacrol | −5.60 ± 0.45 | OA | −4.04 ± 0.75 |
| | | | | | TA | −4.11 ± 0.79 |
| SoTyrR | B-Camphol | −7.10 | Carvacrol | −6.00 ± 0.40 | OA | −5.30 ± 0.22 |
| | Terpinolene | −7.10 | | | | |
| | Carvacrol | −7.10 | | | | |
| TcOctR | Pulegone | −7.00 | Carvacrol | −5.43 ± 0.50 | OA | −3.92 ± 0.58 |

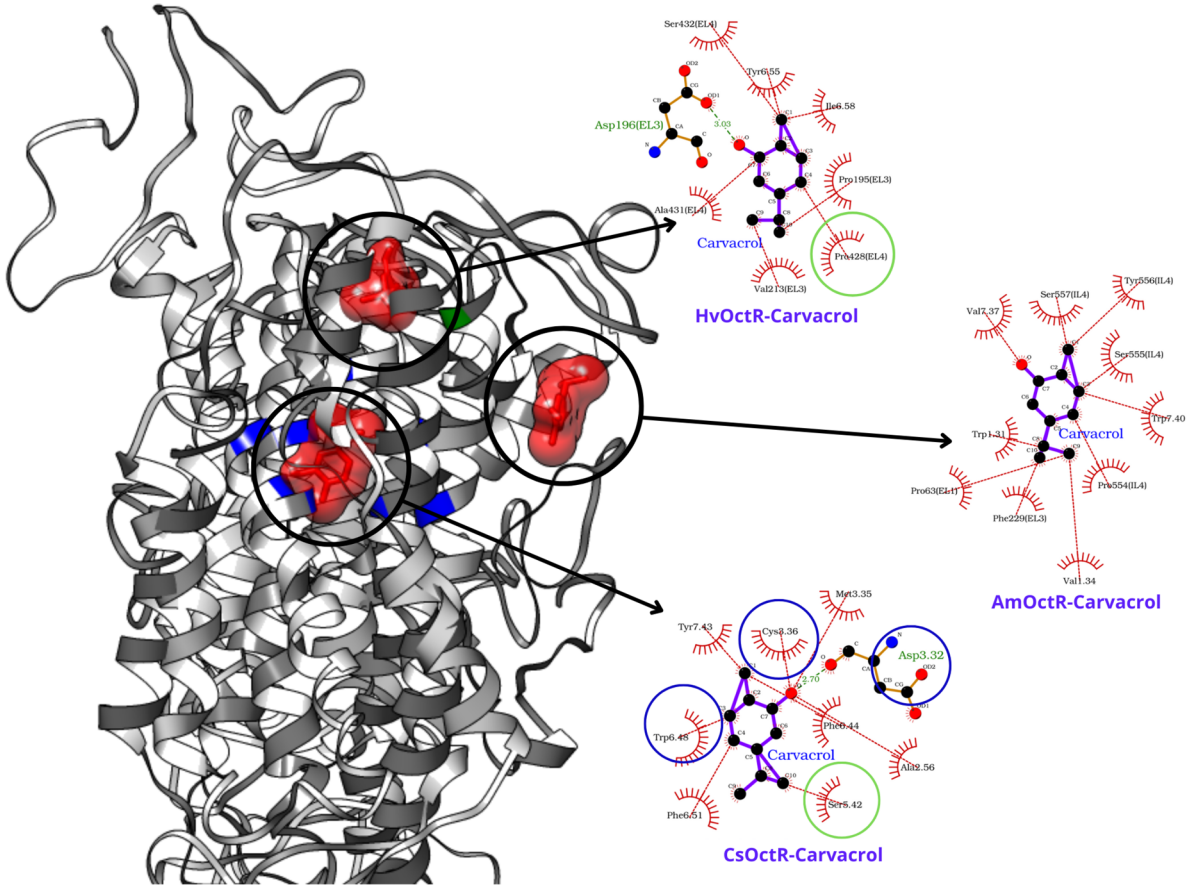


**Figure 5.** Representative illustrations of the three most common interactions observed. Carvacrol ligands are colored in red. Interacting conserved residues near the orthosteric sites are highlighted and encircled in blue. Interacting conserved residues are highlighted and encircled in green.

ligand is ≤8 Å and closely interacted with ≥15% of overall receptor conformations. The common close-interacting residues of carvacrol were compared to the interacting residues in the orthosteric binding pocket and highly conserved residues from the alignment. Generally, three ligand−receptor interaction behaviors were observed: 1) common close interactions with conserved residues near the orthosteric site, 2) common close interactions with conserved residues that are not on the



https://doi.org/10.1021/acsomega.2c06256
ACS Omega 2023, 8, 3861−3871

Table 3. Carvacrol Common Interacting Residues[a]

| Receptor | Carvacrol (967563) Common Interacting Residues |
|---|---|
| AmOctR | Pro63$^{EL1}$, Trp1.31, Phe2.67 |
| BlOctR | Val1.53, Leu2.46, **Ile3.33**, *Val5.39*, *Ser5.42*, Ala5.43, Tyr6.55, Leu7.38, Asn7.49, *Pro7.50* |
| BmOctR | Val2.53, Val2.57, Leu2.58, Pro2.59, Asn2.61, Val2.62, Ser115$^{EL2}$, Trp3.28, **Asp3.32**, *Ile6.40*, **Trp6.48**, **Phe6.51**, Tyr6.55, *Ile7.35*, Ile7.38, **Thr7.39**, Asn7.45, Asn7.49, Ile7.52 |
| CsOctR | Val2.57, Leu3.29, **Asp3.32**, **Val3.33**, **Cys3.36**, *Thr3.37*, Ser4.53, Cys4.57, Trp183$^{EL3}$, Cys185$^{EL3}$, Tyr5.38, Tyr5.41, *Ser5.42*, Ala5.43, Tyr5.48, **Trp6.48**, **Phe6.51**, Tyr6.55, Pro424$^{EL4}$, **Phe7.39** |
| HvOctR | Glu51$^{EL1}$, Ala52$^{EL1}$, Thr55$^{EL1}$, Ala1.36, Asn2.61, Tyr112$^{EL2}$, Ser113$^{EL2}$, Pro200$^{EL3}$, Asp201$^{EL3}$, Val213$^{EL3}$, *Pro6.50*, Tyr6.55, *Pro428$^{EL4}$*, Phe7.37, Ile7.38, Leu7.41 |
| LmTyrR | Leu2.56, Val2.57, Leu3.29, Cys3.31, **Asp3.32**, **Val3.33**, Cys3.35, **Cys3.36**, *Thr3.37*, Ile4.56, Tyr214$^{EL3}$, Gly5.45, *Ser5.46*, **Thr7.39**, Gly7.32, Tyr7.43, Ser7.46 |
| MbOctR | Val2.53, Ala2.54, Val2.57, Leu2.60, Trp118$^{EL2}$, Leu3.29, **Asp3.32**, **Ile3.33**, **Cys3.36**, Leu206$^{EL3}$, Phe5.38, *Val5.39*, Ser5.42, *Ser5.43*, **Trp6.48**, **Phe6.51**, Phe6.52, Tyr6.55, Leu6.56, *Ile7.35*, Ile7.38, **Thr7.39**, Gly7.42, Tyr7.43 |
| PxTyrR | Phe15$^{EL1}$, Tyr21$^{EL1}$, Lys35$^{EL1}$, Phe36$^{EL1}$, Pro37$^{EL1}$, Ser38$^{EL1}$, Trp4.50, Glu198$^{EL3}$, Pro199$^{EL3}$, Thr201$^{EL3}$, Pro202$^{EL3}$, Asn7.36 |
| SlOctTyrR | Thr3.37, *Ser3.38*, *Leu3.41*, Val4.49, Leu4.52, Ser4.53, Ile4.56, Phe5.38, Phe5.41, Ser5.42, Ser5.46, Phe5.47 |
| SoTyrR | Asp2.50, Val2.53, Leu2.56, Val2.57, Trp3.28, Ser3.31, **Asp3.32**, *Cys3.35*, **Cys3.36**, Leu190$^{EL3}$, Ile198$^{EL3}$, *Ser201$^{EL3}$*, Gly203$^{EL3}$, *Ser204$^{EL3}$*, *Phe5.47*, Ile7.35, Ile7.38, **Thr7.39**, Gly7.42, Tyr7.43, Ser7.46 |
| TcOctR | Ser7$^{EL1}$, Ser9$^{EL1}$, Leu186$^{EL3}$, Thr187$^{EL3}$, Val5.39, Ser5.42, *Ser5.43*, *Leu5.51*, **Trp6.48**, **Phe6.51**, Phe6.52, Tyr400$^{EL4}$, Val401$^{EL4}$, Pro404$^{EL4}$, *Lys416$^{EL4}$* |

[a]In bold: highly conserved residues in the orthosteric pocket. In italic: highly conserved residues from the sequence alignment.

orthosteric site, and 3) common close interactions with residues that are not conserved and are not on the orthosteric site. Shown in Figure 5 are representations of these three observed behaviors. The common close-interacting residues of carvacrol in all OARs and TARs investigated are also presented in Table 3. The most common feature of the ligand−receptor interactions, even for the endogenous ligands, is that the involved interacting residues are highly hydrophobic in nature and are usually located in or near the transmembrane helice bundle. This highlights the importance of the hydrophobic nature in ligand binding and interaction.

It can be observed that most of BlOctR, BmOctR, CsOctR, LmTyrR, MbOctR, SoTyrR, and TcOctR interactions with carvacrol involve conserved residues that are in the orthosteric pocket. Most common among these interactions is the involvement of Asp3.32 which forms a hydrogen bond with the ligand. A mutation study revealed that hydrogen bonding of the carboxyl group of this residue with the amine group of tyramine is important in the activation of *B. mori* TAR.[43] Another common interacting residue is Phe6.51, which is identified as a key residue in SoTyrR and monoterpene interaction.[15] Since carvacrol interacts in the same position and with similar residues in BlOctR, BmOctR, CsOctR, LmTyrR, MbOctR, SoTyrR, and TcOctR, this could suggest that carvacrol elicits the same responses and conformational changes in these receptors. Oregano (*Origanum vulgare*) oil, which includes carvacrol as a major component, showed insecticidal activity against grain insects *T. castaneum* and *S. granarius*.[44] A study also showed that carvacrol had a broad insecticidal and acaricidal effect on different insect pests such as the *S. oryzae* and other insects.[45]

Carvacrol interacts predominantly with conserved residues that are not, albeit close, in the orthosteric binding pocket in HvOctR and SlOctTyrR. Molecular docking of amitraz, a known acaricide targeting octopamine receptors, with SoTyrR showed a similar behavior where it bound to a different binding site near the orthosteric pocket.[36] They also identified Asn2.61 as a contact residue for SoTyrR−amitraz interaction, which we also identified as a common close-interacting residue for HvOctR−carvacrol interaction.[36] This difference in the binding position of amitraz and tyramine in SoTyrR was correlated to the difference in the induced conformational change of these ligands and their mechanism of action.[36] In a point mutation study, it was also suggested that an allosteric site might be responsible for the agonist effect of amitraz, and mutations on this site might also reduce the potencies of orthosteric agonists or antagonists, thus inducing resistance.[46] This poses the possibility of carvacrol having an agonist effect on HvOctR and SlOctTyrR, similar to amitraz-dependent action of activation. Carvacrol induced one of the most efficient acute toxic responses in *S. littoralis* and *S. littura*.[47,48]

In AmOctR and PxTyrR, carvacrol interacts with residues that are neither tagged as conserved among the receptors nor located in the orthosteric binding site. Interacting residues are mostly located in the extracellular loops but in different TMs. In the phylogenetic analysis, AmOctR was also seen to have the most distant relationship among the OARs and TARs in this study. In separate studies, carvacrol was also seen to be more toxic to other insects than to the honeybee, *A. mellifera*.[49,50] Carvacrol was also present at low concentrations in bee pollen.[51] Moreover, carvacrol is negative for honey bee toxicity as predicted by admetSAR (http://lmmd.ecust.edu.cn/admetsar2/).[52] These could suggest that carvacrol elicits a different response in AmOctR and PxTyrR compared to the receptors already mentioned. In a recent study, relative insensitivity of the Oct$\beta$2 receptor in *A. mellifera* due to three specific residues is seen to be the rationale behind the amitraz resistance of honeybees compared to mites.[53] Although promising, this study only provides initial insights on the whole picture of the monoterpene-response mechanism of OARs/TARs. More advanced simulations and experimental investigations are direly needed.

Carvacrol, a phenolic monoterpenoid, is present in the essential oils of oregano (*Origanu vulgare*), thyme (*Thymus vulgaris*), pepperwort (*Lepidium flavum*), wild bergamot (*Citrus aurantium* var. *Bergamia Loisel*), and other plants.[54] Interestingly, a study by Hata suggests that intercropping of strawberry plants with oregano and thyme can decrease the population of twospotted spider mites by 50%.[55] Another study, where coffee was intercropped with oregano, resulted in a higher yield and quality production.[56] These suggest that plants containing carvacrol, the top hit ligand, can be utilized by farmers in intercropping to reduce the insect pests mentioned, thereby providing crops of better quality and yield while having minimal effects on beneficial insects such as honeybees.



https://doi.org/10.1021/acsomega.2c06256
ACS Omega 2023, 8, 3861−3871

In conclusion, our results suggest that the IL3 region might be a crucial domain in OAR/TAR identification and unique function which is subject to further studies for confirmation. Ensemble docking revealed the potential of monoterpenes sabinene/camphene, (+)-3-bromocamphor, and B-camphol as species-specific natural-product-based insecticides against HvOctR, PxTyrR, and SoTyrR, respectively. Carvacrol exhibited the highest binding affinity with the majority of the OARs and TARs, although it possesses differences in ligand-induced effects due to the differences of binding sites and interacting residues. Distinctly, AmOctR had the farthest correlation among insect OARs/TARs investigated, and carvacrol interacted with the nonconserved residues of the Western honeybee (*A. mellifera*) OAR and Asian swallowtail butterfly (*P. xuthus*) TAR. These suggest that utilization of carvacrol-producing plants could be explored as an insecticide or repellent against the insects in this study while being potentially nonharmful to the pollinating insects Western honeybee and Asian swallowtail butterfly. This computational approach aids in further understanding the specificity of monoterpene compounds as potential species-specific and natural-product-based insecticides to insect pests. Further dynamic and/or *in vitro* and *in vivo* studies are recommended.

## MATERIALS AND METHODS

**Uniprot Sequence Retrieval and Phylogenetic Analysis.** The FASTA sequence of the 11 insect receptors was sourced from the Universal Protein Resource (UniProt) web server (https://www.uniprot.org/) (Table S7). UniProt is a web database that contains a comprehensive resource of protein sequences and protein annotation.[57] The sequences of each were aligned to each other using the NCBI BLAST tool.[58] The phylogenetic tree was generated using the maximum likelihood method implemented in MEGA 7.0 software with the JTT model and pairwise gap deletion option.[59] Bootstrap analysis was conducted with 100 iterations.

**Homology Modeling.** Due to the absence of insect OAR and TAR crystal structures in databases, homology modeling was employed to obtain a representative protein structure. The amino acid sequences were obtained from UniProt.[57] The I-TASSER Web server (https://zhanggroup.org/I-TASSER/) was used to generate the 3D models of each OAR/TAR.[27] Default settings of I-TASSER were used. The most optimal 3D model based on the C-score and TM-score for each receptor was chosen for succeeding procedures.

**Structure Preparation and CGMD Simulations.** Coarse-grained molecular dynamics (CGMD) simulations were employed to obtain representative ensemble structures for docking. All systems used in CGMD were built in the CHARMM-GUI Martini Bilayer Builder.[60] Eleven systems were prepared, each containing the coarse-grained version of the receptor embedded in a 1-palmitoyl-2-oleoyl-*sn*-glycero-3-phosphocholine (POPC) lipid bilayer. Lipid content was set to a 1:1 ratio of upper and lower leaflet and spanned a 220 × 220 Å$^2$ area. The minimum water height above and below the lipid system was maintained at the default 22.5 Å. A sufficient number of ions were added to neutralize each system (Table S8).

CGMD was performed in GROMACS 2020.6, following the standard Martini protocol.[61,62] The minimization phase was conducted with a steepest descent algorithm and lasted 10,000 steps. This was succeeded by an NPT equilibration step. Pressure was controlled at 1 bar using a semi-isotropic Berendsen barostat with a coupling constant of 5 ps.[63] Temperature was set at 303.15 K through the velocity rescaling thermostat with a coupling constant of 1 ps.[64] Periodic boundary conditions and the particle-mesh-Ewald method were employed for electrostatic interaction calculations.[65] The leapfrog algorithm was applied for the numerical integration of the classical equations of motion.[66] An NPT production run of 1 $\mu$s was executed with an integration time step of 20 fs. Structure coordinates were written in the output trajectory every 100 ps, which generated 10,000 frames by the end of the simulation.

**Structure Clustering and Backmapping.** Structure clustering was conducted using the pytraj clustering algorithm. With the CGMD trajectory as the input, similar conformations were grouped, and representative structures were generated. The criterion for grouping is an optimal RMSD value cutoff ranging from 2.0 to 2.5 Å. Pytraj also generated network representations, which were visualized using the Python graph-tool (http://graph-tool.skewed.de/). The representative structures were backmapped using the Martini backmapping protocol.[67]

**Structure Alignment.** The first frames of each protein receptor in the production run of CGMD simulations were backmapped and were used for structural comparison and alignment in UCSF Chimera.[68] In the MatchMaker tool, the Needleman−Wunsch alignment algorithm and BLOSUM-62 matrix were used to align all the protein structures using the most optimal model (based on C-score and TM-score) from homology modeling as the reference structure. The superimposition was iterated by pruning long atom pairs until no pair exceeds 2 Å. After superimposition, a structure-based multiple-sequence alignment was performed using the Match → Align tool. The residue−residue distance cutoff was set to 5 Å, and circular permutations were allowed. The alignment was iterated three times. Highly conserved regions were visualized using WebLogo.[69]

**Ensemble Docking.** The backmapped representative structures and 35 monoterpenes were subjected to ensemble docking. All ligand structures were obtained from the ZINC database and were converted and prepared in 3D (Table S9).[70,71] The endogenous ligands octopamine and tyramine with the OARs and TARs were used as control systems. In both the ligand and receptor preparation, Gasteiger charges were added. In ligand preparation, all backbones were set as rotatable and active while leaving amide and guanidinium groups nonrotatable and inactive. Ensemble docking was executed using AutoDock Vina.[72] All exhaustiveness were set to 16 to give adequate run time given the atom size and flexibility of the ligands. For the docking of monoterpene compounds, a search box size of 40 × 40 × 40 Å$^3$ was used and centered in the extracellular loops to cover the whole region including the upper transmembrane helices (Table S6). For the endogenous ligand docking, a search box size of 20 × 20 × 20 Å$^3$ was used and centered in the conserved Asp residue in TM3 located near the orthosteric binding pocket which is already known to make consensus contacts with endogenous ligands.[40] The average binding energies were reported in kcal/mol. The top hits and key interacting residues were determined and visualized using Ligplot+.[73]


https://doi.org/10.1021/acsomega.2c06256
ACS Omega 2023, 8, 3861−3871

## ■ ASSOCIATED CONTENT

### Supporting Information

The Supporting Information is available free of charge at https://pubs.acs.org/doi/10.1021/acsomega.2c06256.

List of C-scores and TM-scores of the OAR/TAR models generated by I-TASSER; results of secondary structure superposition in the Chimera Matchmaker tool using CsOctR as a reference structure; RMSD (Å) measurement of structure-based sequence alignment obtained from Chimera Match → Align; equivalent residue numbers in conserved positions using the Ballesteros−Weinstein naming scheme; contact residues at orthosteric pockets of the 11 insect receptors based on the Ballesteros−Weinstein naming scheme; residues where the grid boxes were centered; receptor abbreviations and UniProt accession codes; system components in CGMD; monoterpene ligands used and their ZINC ID (Tables S1−S9); and highly conserved residues, highlighted in peach, from structural alignment done in UCSF Chimera (Figure S1) (PDF)

## ■ AUTHOR INFORMATION


### Corresponding Author

**Ricky B. Nellas** − *Institute of Chemistry, College of Science, University of the Philippines Diliman, Quezon City 1101, Philippines*; Email: rbnellas@up.edu.ph

### Authors

**Almira B. Ocampo** − *Institute of Chemistry, College of Science, University of the Philippines Diliman, Quezon City 1101, Philippines*

**Joseph Gregory Z. Cabinta** − *Institute of Chemistry, College of Science, University of the Philippines Diliman, Quezon City 1101, Philippines*; orcid.org/0000-0003-0544-7648

**Hyvi Valerie J. Padilla** − *Institute of Chemistry, College of Science, University of the Philippines Diliman, Quezon City 1101, Philippines*

**Eizadora T. Yu** − *Marine Science Institute, College of Science, University of the Philippines Diliman, Quezon City 1101, Philippines*

Complete contact information is available at: https://pubs.acs.org/10.1021/acsomega.2c06256


### Notes

The authors declare no competing financial interest.

## ■ ACKNOWLEDGMENTS

The authors thank the Department of Science and Technology-Advanced Science and Technology Institute (DOST-ASTI) Computing and Archiving Research Environment (CoARE) Facility, the University of the Philippines (UP) Diliman College of Science Computational Science Research Center (CSRC), and the UP Office of the Vice President for Academic Affairs-Emerging Interdisciplinary Research (EIDR) Program for the computing resources. This study was funded by the Department of Agriculture - Biotechnology Program (Grant: DABIOTECH - R1605). A.B.O. would like to acknowledge the Department of Science and Technology Science Education Institute for her academic scholarship.

## ■ REFERENCES


(1) Sparks, T. C.; Lorsbach, B. A. Perspectives on the agrochemical industry and agrochemical discovery. *Pest Manage. Sci.* **2017**, *73*, 672−677.

(2) Hill, C. A.; Sharan, S.; Watts, V. J. Genomics, GPCRs and new targets for the control of insect pests and vectors. *Curr. Opin. Insect Sci.* **2018**, *30*, 99−106.

(3) Vaidehi, N.; Floriano, W. B.; Trabanino, R.; Hall, S. E.; Freddolino, P.; Choi, E. J.; Zamanakos, G.; Goddard, W. A. Prediction of structure and function of G protein-coupled receptors. *Proc. Natl. Acad. Sci. U. S. A.* **2002**, *99*, 12622−12627.

(4) Liu, N.; Li, T.; Wang, Y.; Liu, S. G-protein coupled receptors (GPCRs) in insects−A potential target for new insecticide development. *Molecules* **2021**, *26*, 2993.

(5) Roeder, T. A new octopamine receptor class in locust nervous tissue, the octopamine 3 (OA3) receptor. *Life Sci.* **1992**, *50*, 21−28.

(6) Evans, P. D.; Maqueira, B. Insect octopamine receptors: a new classification scheme based on studies of cloned Drosophila G-protein coupled receptors. *Invertebr. Neurosci.* **2005**, *5*, 111−118.

(7) Alkema, M. J.; Hunter-Ensor, M.; Ringstad, N.; Horvitz, H. R. Tyramine functions independently of octopamine in the Caenorhabditis elegans nervous system. *Neuron* **2005**, *46*, 247−260.

(8) García-Lara, S.; Saldivar, S. O. S. In *Encyclopedia of Food and Health*; Caballero, B., Finglas, P. M., Toldrá, F., Eds.; Academic Press, 2016; pp 432−436.

(9) Cartea, M. E.; Francisco, M.; Lema, M.; Soengas, P.; Velasco, P. Resistance of cabbage (Brassica oleracea capitata group) crops to Mamestra brassicae. *J. Econ. Entomol.* **2010**, *103*, 1866−1874.

(10) Bokonon-Ganta, A. H.; McQuate, G. T.; Messing, R. H. Natural establishment of a parasitoid complex on Bactrocera latifrons (Diptera: Tephritidae) in Hawaii. *Biol. Control* **2007**, *42*, 365.

(11) Starỳ, P.; Pike, K. S. In *Biodiversity in agroecosystems*; Collins, W. W., Qualset, C. O., Eds.; CRC Press, 1998; Chapter 4, pp 49−67.

(12) Chen, Y.; Evans, J.; Feldlaufer, M. Horizontal and vertical transmission of viruses in the honey bee, Apis mellifera. *J. Invertebr. Pathol.* **2006**, *92*, 152−159.

(13) Roeder, T. Tyramine and octopamine: ruling behavior and metabolism. *Annu. Rev. Entomol.* **2005**, *50*, 447−477.

(14) Roeder, T.; Degen, J.; Dyczkowski, C.; Gewecke, M. In *New Strategies in Locust Control*; Krall, S., Peveling, R., Ba Diallo, D., Eds.; Birkhäuser, 1997; pp 219−223.

(15) Ocampo, A. B.; Braza, M. K. E.; Nellas, R. B. The interaction and mechanism of monoterpenes with tyramine receptor (SoTyrR) of rice weevil (Sitophilus oryzae). *SN Appl. Sci.* **2020**, *2*, 1592.

(16) Dacanay, F. N. D.; Ladra, M.; Junio, H. A.; Nellas, R. B. Molecular affinity of mabolo extracts to an octopamine receptor of a fruit fly. *Molecules* **2017**, *22*, 1677.

(17) Enan, E. Insecticidal activity of essential oils: octopaminergic sites of action. *Comp. Biochem. Physiol., Part C: Toxicol. Pharmacol.* **2001**, *130*, 325−337.

(18) Liu, Z.; Li, Q. X.; Song, B. Pesticidal Activity and Mode of Action of Monoterpenes. *J. Agric. Food. Chem.* **2022**, *70*, 4556−4571.

(19) Yeom, H.-J.; Jung, C.-S.; Kang, J.; Kim, J.; Lee, J.-H.; Kim, D.-S.; Kim, H.-S.; Park, P.-S.; Kang, K.-S.; Park, I.-K. Insecticidal and acetylcholine esterase inhibition activity of Asteraceae plant essential oils and their constituents against adults of the German cockroach (Blattella germanica). *J. Agric. Food. Chem.* **2015**, *63*, 2241−2248.

(20) Soares Rodrigues, G. C.; dos Santos Maia, M.; Muratov, E. N.; Scotti, L.; Scotti, M. T. Quantitative Structure-Activity Relationship Modeling and Docking of Monoterpenes with Insecticidal Activity Against Reticulitermes chinensis Snyder and Drosophila melanogaster. *J. Agric. Food. Chem.* **2020**, *68*, 4687−4698.

(21) Abdelgaleil, S. A. M.; Gad, H. A.; Ramadan, G. R.; El-Bakry, A. M.; El-Sabrout, A. M. Monoterpenes: chemistry, insecticidal activity against stored product insects and modes of action—a review. *Int. J. Pest Manage.* **2021**, 1−23.

(22) Enan, E. E. Molecular response of Drosophila melanogaster tyramine receptor cascade to plant essential oils. *Insect Biochem. Mol. Biol.* **2005**, *35*, 309−321.

(23) Gross, A. D.; Temeyer, K. B.; Day, T. A.; de León, A. A. P.; Kimber, M. J.; Coats, J. R. Interaction of plant essential oil terpenoids with the southern cattle tick tyramine receptor: A potential biopesticide target. *Chem. Biol. Interact.* **2017**, *263*, 1−6.
(24) Finetti, L.; Ferrari, F.; Caló, G.; Cassanelli, S.; De Bastiani, M.; Civolani, S.; Bernacchia, G. Modulation of Drosophila suzukii type 1 tyramine receptor (DsTAR1) by monoterpenes: a potential new target for next generation biopesticides. *Pestic. Biochem. Physiol.* **2020**, *165*, 104549.
(25) Saad, M. M.; Abou-Taleb, H. K.; Abdelgaleil, S. A. Insecticidal activities of monoterpenes and phenylpropenes against Sitophilus oryzae and their inhibitory effects on acetylcholinesterase and adenosine triphosphatases. *Appl. Entomol. Zool.* **2018**, *53*, 173−181.
(26) Seo, S.-M.; Kim, J.; Lee, S.-G.; Shin, C.-H.; Shin, S.-C.; Park, I.-K. Fumigant antitermitic activity of plant essential oils and components from ajowan (Trachyspermum ammi), allspice (Pimenta dioica), caraway (Carum carvi), dill (Anethum graveolens), geranium (Pelargonium graveolens), and litsea (Litsea cubeba) oils against Japanese termite (Reticulitermes speratus Kolbe). *J. Agric. Food. Chem.* **2009**, *57*, 6596−6602.
(27) Yang, J.; Zhang, Y. I-TASSER server: new development for protein structure and function predictions. *Nucleic Acids Res.* **2015**, *43*, W174−W181.
(28) Cavasotto, C. N.; Phatak, S. S. Homology modeling in drug discovery: current trends and applications. *Drug Discovery Today* **2009**, *14*, 676−683.
(29) Davies, M. N.; Gloriam, D. E.; Secker, A.; Freitas, A. A.; Mendao, M.; Timmis, J.; Flower, D. R. Proteomic applications of automated GPCR classification. *Proteomics* **2007**, *7*, 2800−2814.
(30) Worth, C. L.; Kleinau, G.; Krause, G. Comparative sequence and structural analyses of G-protein-coupled receptor crystal structures and implications for molecular models. *PloS one* **2009**, *4*, e7011.
(31) Daura, X.; Gademann, K.; Jaun, B.; Seebach, D.; Van Gunsteren, W. F.; Mark, A. E. Peptide folding: when simulation meets experiment. *Angew. Chem., Int. Ed.* **1999**, *38*, 236−240.
(32) Frauenfelder, H.; Leeson, D. T. The energy landscape in non-biological and biological molecules. *Nat. Struct. Biol.* **1998**, *5*, 757−759.
(33) Phillips, T. W.; Throne, J. E. Biorational approaches to managing stored-product insects. *Annu. Rev. Entomol.* **2010**, *55*, 375−397.
(34) Finetti, L.; Roeder, T.; Calo, G.; Bernacchia, G. The insect type 1 tyramine receptors: from structure to behavior. *Insects* **2021**, *12*, 315.
(35) Yarnitzky, T.; Levit, A.; Niv, M. Y. Homology modeling of G-protein-coupled receptors with X-ray structures on the rise. *Curr. Opin. Drug Discovery Dev.* **2010**, *13*, 317−325.
(36) Braza, M. K. E.; Gazmen, J. D. N.; Yu, E. T.; Nellas, R. B. Ligand-induced conformational dynamics of a tyramine receptor from Sitophilus oryzae. *Sci. Rep.* **2019**, *9*, 1−14.
(37) Huang, H.; Huang, H.; Tao, Y.-X. Functions of the DRY motif and intracellular loop 2 of human melanocortin 3 receptor. *J. Mol. Endocrinol* **2014**, *53*, 319−319.
(38) Rovati, G. E.; Capra, V.; Neubig, R. R. The highly conserved DRY motif of class A G protein-coupled receptors: beyond the ground state. *Mol. Pharmacol.* **2007**, *71*, 959−964.
(39) Kobilka, B. K. G protein coupled receptor structure and activation. *Biochimica et Biophysica Acta (BBA)-Biomembranes* **2007**, *1768*, 794−807.
(40) Venkatakrishnan, A. J.; Deupi, X.; Lebon, G.; Tate, C. G.; Schertler, G. F.; Babu, M. M. Molecular signatures of G-protein-coupled receptors. *Nature* **2013**, *494*, 185−194.
(41) Ballesteros, J. A.; Weinstein, H. *Methods in neurosciences*; Elsevier, 1995; Vol. *25*, pp 366−428.
(42) Isberg, V.; de Graaf, C.; Bortolato, A.; Cherezov, V.; Katritch, V.; Marshall, F. H.; Mordalski, S.; Pin, J.-P.; Stevens, R. C.; Vriend, G.; et al. Generic GPCR residue numbers−aligning topology maps while minding the gaps. *Trends Pharmacol. Sci.* **2015**, *36*, 22−31.
(43) Ohta, H.; Utsumi, T.; Ozoe, Y. Amino acid residues involved in interaction with tyramine in the Bombyx mori tyramine receptor. *Insect Mol. Biol.* **2004**, *13*, 531−538.
(44) Can Baser, K. H. Biological and Pharmacological Activities of Carvacrol and Carvacrol Bearing Essential Oils. *Curr. Pharm. Des.* **2008**, *14*, 3106−3119.
(45) Ahn, Y.-J.; Lee, S.-B.; Lee, H.-S.; Kim, G.-H. Insecticidal and Acaricidal Activity of Carvacrol and β-Thujaplicine Derived from Thujopsis dolabrata var. hondai Sawdust. *J. Chem. Ecol.* **1998**, *24*, 81−90.
(46) Takata, M.; Misato, S.; Ozoe, F.; Ozoe, Y. A point mutation in the β-adrenergic-like octopamine receptor: possible association with amitraz resistance. *Pest. Manage. Sci.* **2020**, *76*, 3720−3728.
(47) Pavela, R. Acute and synergistic effects of monoterpenoid essential oil compounds on the larvae of Spodoptera littoralis. *J. Biopestic.* **2010**, *3*, 573.
(48) Hummelbrunner, L. A.; Isman, M. B. Acute, sublethal, antifeedant, and synergistic effects of monoterpenoid essential oil compounds on the tobacco cutworm, Spodoptera litura (Lep., Noctuidae). *J. Agric. Food. Chem.* **2001**, *49*, 715−720.
(49) Ellis, M. D. Toxic effects of monoterpenoids in the honey bee, Apis mellifera L., and its tracheal mite parasite, Acarapis woodi (Rennie). *Ph.D. thesis*, The University of Nebraska: Lincoln, NE.
(50) Ellis, M. D.; Baxendale, F. P. Toxicity of Seven Monoterpenoids to Tracheal Mites (Acari: Tarsonemidae) and Their Honey Bee (Hymenoptera: Apidae) Hosts When Applied as Fumigants. *J. Econ. Entomol.* **1997**, *90*, 1087−1091.
(51) Ares, A. M.; Nozal, M. J.; Bernal, J. L.; Bernal, J. Simultaneous determination of carvacrol and thymol in bee pollen by using a simple and efficient solvent extraction method and gas chromatography-mass spectrometry. *J. Pharm. Biomed. Anal.* **2020**, *181*, 113124.
(52) Yang, H.; Lou, C.; Sun, L.; Li, J.; Cai, Y.; Wang, Z.; Li, W.; Liu, G.; Tang, Y. admetSAR 2.0: web-service for prediction and optimization of chemical ADMET properties. *Bioinformatics* **2019**, *35*, 1067−1069.
(53) Guo, L.; Fan, X.-y.; Qiao, X.; Montell, C.; Huang, J. An octopamine receptor confers selective toxicity of amitraz on honeybees and Varroa mites. *Elife* **2021**, *10*, e68268.
(54) Sharifi-Rad, M.; Varoni, E. M.; Iriti, M.; Martorell, M.; Setzer, W. N.; del Mar Contreras, M.; Salehi, B.; Soltani-Nejad, A.; Rajabi, S.; Tajbakhsh, M.; et al. Carvacrol and human health: A comprehensive review. *Phytother. Res.* **2018**, *32*, 1675−1687.
(55) Dittrich, F.; Iserloh, T.; Treseler, C.-H.; Hüppi, R.; Ogan, S.; Seeger, M.; Thiele-Bruhn, S. Crop diversification in viticulture with aromatic plants: Effects of intercropping on grapevine productivity in a steep-slope vineyard in the Mosel Area, Germany. *Agriculture* **2021**, *11*, 95.
(56) Bustos, A. P.; Pohlan, H. J.; Schulz, M. Interaction between coffee (Coffea arabica L.) and intercropped herbs under field conditions in the Sierra Norte of Puebla, Mexico. *JARTS* **2008**, *109*, 85−93.
(57) Consortium, U. UniProt: a worldwide hub of protein knowledge. *Nucleic Acids Res.* **2019**, *47*, D506−D515.
(58) Altschul, S. F.; Gish, W.; Miller, W.; Myers, E. W.; Lipman, D. J. Basic local alignment search tool. *J. Mol. Biol.* **1990**, *215*, 403−410.
(59) Kumar, S.; Stecher, G.; Li, M.; Knyaz, C.; Tamura, K. MEGA X: molecular evolutionary genetics analysis across computing platforms. *Mol. Biol. Evol.* **2018**, *35*, 1547.
(60) Qi, Y.; Ingólfsson, H. I.; Cheng, X.; Lee, J.; Marrink, S. J.; Im, W. CHARMM-GUI Martini Maker for Coarse-Grained Simulations with the Martini Force Field. *J. Chem. Theory Comput.* **2015**, *11*, 4486−4494.
(61) Abraham, M. J.; Murtola, T.; Schulz, R.; Páll, S.; Smith, J. C.; Hess, B.; Lindahl, E. GROMACS: High performance molecular simulations through multi-level parallelism from laptops to supercomputers. *SoftwareX* **2015**, *1−2*, 19−25.
(62) Marrink, S. J.; Marrink, S. J.; Risselada, H. J.; Yefimov, S.; Tieleman, D. P.; de Vries, A. H. The MARTINI Force Field: Coarse


https://doi.org/10.1021/acsomega.2c06256
ACS Omega 2023, 8, 3861−3871

Grained Model for Biomolecular Simulations. *J. Phys. Chem. B* **2007**, *111*, 7812.
(63) Berendsen, H. J. C.; Postma, J. P. M.; van Gunsteren, W. F.; DiNola, A.; Haak, J. R. Molecular dynamics with coupling to an external bath. *J. Chem. Phys.* **1984**, *81*, 3684−3690.
(64) Bussi, G.; Donadio, D.; Parrinello, M. Canonical sampling through velocity rescaling. *J. Chem. Phys.* **2007**, *126*, 014101.
(65) Darden, T.; York, D.; Pedersen, L. Particle mesh Ewald: An N · log (N) method for Ewald sums in large systems. *J. Chem. Phys.* **1993**, *98*, 10089−10092.
(66) Van Gunsteren, W. F.; Berendsen, H. J. A leap-frog algorithm for stochastic dynamics. *Mol. Simul.* **1988**, *1*, 173−185.
(67) Wassenaar, T. A.; Pluhackova, K.; Böckmann, R. A.; Marrink, S. J.; Tieleman, D. P. Going backward: a flexible geometric approach to reverse transformation from coarse grained to atomistic models. *J. Chem. Theory Comput.* **2014**, *10*, 676−690.
(68) Pettersen, E. F.; Goddard, T. D.; Huang, C. C.; Couch, G. S.; Greenblatt, D. M.; Meng, E. C.; Ferrin, T. E. UCSF Chimera—a visualization system for exploratory research and analysis. *J. Comput. Chem.* **2004**, *25*, 1605−1612.
(69) Crooks, G. E.; Hon, G.; Chandonia, J.-M.; Brenner, S. E. WebLogo: a sequence logo generator. *Genome Res.* **2004**, *14*, 1188−1190.
(70) Irwin, J. J.; Sterling, T.; Mysinger, M. M.; Bolstad, E. S.; Coleman, R. G. ZINC: a free tool to discover chemistry for biology. *J. Chem. Inf. Model.* **2012**, *52*, 1757−1768.
(71) Morris, G. M.; Huey, R.; Lindstrom, W.; Sanner, M. F.; Belew, R. K.; Goodsell, D. S.; Olson, A. J. AutoDock4 and AutoDockTools4: Automated docking with selective receptor flexibility. *J. Comput. Chem.* **2009**, *30*, 2785−2791.
(72) Trott, O.; Olson, A. J. AutoDock Vina: improving the speed and accuracy of docking with a new scoring function, efficient optimization, and multithreading. *J. Comput. Chem.* **2009**, *31*, 455−461.
(73) Laskowski, R. A.; Swindells, M. B. LigPlot+: multiple ligand−protein interaction diagrams for drug discovery. *J. Chem. Inf. Model.* **2011**, *51*, 2778−2786.



https://doi.org/10.1021/acsomega.2c06256
*ACS Omega* 2023, 8, 3861−3871